

# 11

## Charged-current reactions

Charged-current interactions are the most frequent and occur in decays, as well as in particle reactions. They have been analyzed in many books, especially those written before 1970. Charged-current interactions, especially decays, were instrumental in establishing properties of the currents. We can classify them according to the degree of our theoretical understanding. The simplest reactions are purely leptonic. They are relatively simple to calculate, because the couplings of leptons to currents are precisely known and, now that the theory is renormalizable, we can include loop corrections. Some leptonic reactions were presented in Chapter 8. We shall not study them further.

The next class of reactions consists of the semileptonic ones, which can also be treated successfully with various theoretical methods. They involve a single coupling of the currents to hadrons, which can be understood at low energy and/or at low momentum transfer in terms of form factors. They are also understood at high energies in terms of the short-distance behavior of the currents. We shall study several processes in this chapter: deep inelastic scattering and quasi-elastic scattering.

Non-leptonic interactions are the most difficult to analyze. They do not include any leptons and involve both strong and weak interactions. The interplay between the two interactions is still a developing field of research.

### 11.1 Deep inelastic scattering

High-energy neutrino interactions have been used to probe the inner structure of protons and neutrons: these studies were crucial for establishing the quark substructure of matter and giving quantitative support to the field theory of quark interactions (quantum chromodynamics). In Chapter 10 we described the general structure of the cross sections and some consequences of the scaling phenomenon.

Then we showed that the general features can be explained in terms of the quark–parton model. Many more properties and correlations with other reactions have been understood and we discuss them here in greater detail.

### 11.1.1 Scaling and the charge of the quarks

The electroproduction reactions couple to the charge of the quarks, in contrast to the neutrino reactions, which couple to the weak isospin. Comparison of the two processes gives an indication regarding the charge of the constituents.

The electroproduction cross section is

$$\begin{aligned} \frac{d\sigma}{dQ^2 dv} &= \frac{4\pi\alpha^2}{Q^4} \int dx \delta\left(v - \frac{Q^2}{2Mx}\right) \sum_i e_i^2 [q_i(x) + \bar{q}_i(x)] \\ &= \frac{4\pi\alpha^2}{Q^4} \frac{x}{v} \sum_i e_i^2 [q_i(x) + \bar{q}_i(x)], \end{aligned} \tag{11.1}$$

with the normalization chosen to reproduce the Mott cross section. We obtain the structure function

$$F_2^{\text{ep}}(x) = x \left\{ \frac{4}{9} [u(x) + \bar{u}(x)] + \frac{1}{9} [d(x) + \bar{d}(x) + s(x) + \bar{s}(x)] \right\}, \tag{11.2}$$

where  $u(x)$ ,  $d(x)$ ,  $\bar{u}(x)$ , and  $\bar{d}(x)$  are the quark distribution functions in the proton. Similar equations hold for electron–neutron scattering, in which the exchanges  $u \leftrightarrow d$  and  $\bar{u} \leftrightarrow \bar{d}$  take place. The structure function on an isoscalar target is the average over protons and neutrons,

$$F_2^{\text{eN}}(x) = x \left\{ \frac{5}{18} [u(x) + \bar{u}(x) + d(x) + \bar{d}(x)] + \frac{1}{9} [s(x) + \bar{s}(x)] \right\}, \tag{11.3}$$

where the factor of 5/18 follows directly from the fractional charges of the quarks.

For neutrino-induced reactions the structure functions are expressed in terms of the quark distributions

$$F_2^{\nu\text{p}}(x) = 2x [q_i(x) + \bar{q}_i(x)], \tag{11.4}$$

$$F_2^{\nu\text{p}}(x) = 2x F_1^{\nu\text{p}}(x) \quad (\text{Callan and Gross, 1969}), \tag{11.5}$$

$$xF_3^{\nu\text{p}}(x) = 2x [q_i(x) - \bar{q}_i(x)]. \tag{11.6}$$

For neutrinos the following elementary processes are possible:

$$\nu d \rightarrow \mu^- u,$$

$$\nu \bar{u} \rightarrow \mu^- \bar{d};$$

and for antineutrinos

$$\begin{aligned}\bar{\nu}u &\rightarrow \mu^+d, \\ \bar{\nu}\bar{d} &\rightarrow \mu^+\bar{u}.\end{aligned}$$

We shall assume in this section that the Cabbibo angle is zero, so that scatterings from strange quarks are neglected. Then we obtain the structure functions

$$\begin{aligned}F_2^{\nu p}(x) &= 2x[d(x) + \bar{u}(x)], \\ F_2^{\bar{\nu}p}(x) &= 2x[\bar{d}(x) + u(x)] = f_2^{\nu n}(x)\end{aligned}\quad (11.7)$$

and, for isoscalar targets,

$$F_2^{\nu N}(x) = x[u(x) + d(x) + \bar{u}(x) + \bar{d}(x)] \quad (11.8)$$

and

$$xF_3^{\nu N}(x) = x[u(x) + d(x) - \bar{u}(x) - \bar{d}(x)]. \quad (11.9)$$

Since the strange-quark structure functions  $s(x)$  and  $\bar{s}(x)$  are relatively small, we can neglect them and obtain from Eqs. (11.3) and (11.8) the ratio

$$\frac{F_2^{eN}(x)}{F_2^{\nu N}(x)} = \frac{5}{18}. \quad (11.10)$$

The ratio measures the average charge of the quarks and it indicates that the charges of the constituents are fractional. These and other relations have shown that the constituents of hadrons which couple in deep inelastic scattering carry the quantum numbers of the quarks.

### 11.1.2 Spin of the quarks

In the V–A theory all fermions participate in the weak interactions as left-handed particles and all antifermions as right-handed particles. For antineutrino–quark scattering, helicity conservation requires that the process in the center-of-mass frame vanishes at  $\theta_{\text{cm}} = 180^\circ$  as shown in Fig. 11.1.

The cross section has the angular dependence

$$\frac{d\sigma^{\bar{\nu}q}}{d\cos\theta_{\text{cm}}} \propto (1 + \cos\theta_{\text{cm}})^2. \quad (11.11)$$

The center-of-mass angle  $\theta_{\text{cm}}$  is related to the laboratory energies by

$$\frac{1 + \cos\theta_{\text{cm}}}{2} = \frac{E_\mu}{E_\nu} = 1 - y, \quad (11.12)$$

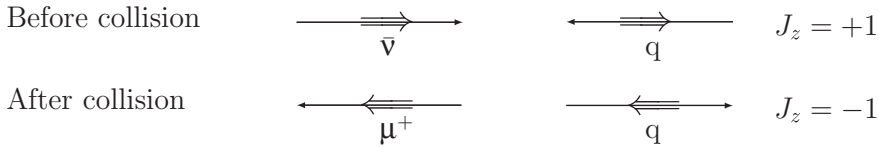


Figure 11.1. Production of a forbidden configuration by helicity conservation in antineutrino–quark scattering.

Table 11.1. Angular dependences of the reactions

Process	$J_z$	$y$ Dependence
$\nu q, \bar{\nu} \bar{q} : \begin{smallmatrix} \leftarrow \\ \nu \end{smallmatrix} \begin{smallmatrix} \rightarrow \\ q \end{smallmatrix}$	0	1
$\nu \bar{q}, \bar{\nu} q : \begin{smallmatrix} \leftarrow \\ \nu \end{smallmatrix} \begin{smallmatrix} \leftarrow \\ \bar{q} \end{smallmatrix}$	1	$(1 - y)^2$

which is easily obtained by evaluating the ratio  $k' \cdot p / (k \cdot p)$  in the center-of-mass system. In this pictorial manner we understand the  $y$  dependence of the cross section:

$$\frac{d\sigma^{\bar{\nu}q}}{dy} \propto (1 - y)^2. \tag{11.13}$$

A similar study of the reaction

$$\nu + d \rightarrow \mu^- + u \tag{11.14}$$

shows that there is no reason for the cross section to vanish in any direction. In this way we construct Table 11.1.

The cross sections in terms of the various species attain the form with  $q(x)$  and  $\bar{q}(x)$  contributions from spin- $\frac{1}{2}$  constituents and  $k(x)$  distributions for spin-zero constituents:

$$\frac{d\sigma^{\nu N}}{dx dy} = \frac{G^2 M E_\nu}{\pi} x [q(x) + (1 - y)^2 \bar{q}(x) + (1 - y)k(x)], \tag{11.15}$$

$$\frac{d\sigma^{\bar{\nu} N}}{dx dy} = \frac{G^2 M E_{\bar{\nu}}}{\pi} x [(1 - y)^2 q(x) + \bar{q}(x) + (1 - y)k(x)]. \tag{11.16}$$

The experimental results indicate that the scattering occurs on spin- $\frac{1}{2}$  constituents and that the content of scalar constituents is very small. The  $y$  distribution for antineutrinos is not exactly zero at  $y = 1$  because protons and neutrons contain a sea of quark–antiquark pairs in addition to their valence quarks. These pairs are created by the emission of vector particles, the gluons, which also bind the quarks into hadrons.

### 11.1.3 Sum rules

In the quark parton model, the distribution functions indicate how the quantum numbers are distributed within hadrons. Thus integrals of distribution functions must reproduce the quantum numbers of the target. For instance,  $\int_0^1 s(x)dx$  gives the probability of finding a strange quark, with any momentum, within a proton. Since the proton has zero strangeness,

$$\int_0^1 [s(x) - \bar{s}(x)]dx = 0. \quad (11.17)$$

Similarly we can compute the baryon number and isospin of a proton:

$$\frac{1}{3} \int_0^1 [u + d - \bar{u} - \bar{d}]dx = 1 \quad (\text{baryon}), \quad (11.18)$$

$$\int_0^1 [(u - d) - (\bar{u} - \bar{d})]dx = 1 \quad (\text{isospin}). \quad (11.19)$$

Such relations are known as sum rules and have been determined by combining data from various processes.

A good example is the Adler (1965) sum rule

$$S_A = \frac{1}{2} \int [F_2^{\bar{\nu}p}(x) - F_2^{\nu p}(x)] \frac{dx}{x} = 1, \quad (11.20)$$

which follows from the isospin relation in (11.19). The Adler sum rule follows from current algebra and it must be valid for each value of  $Q^2$ . In fact, it is a consequence of the commutator of two isospin charges and as such is very reliable. Experimental results give the value

$$S_A = 1.08 \pm 0.20, \quad (11.21)$$

which is in good agreement but the error is relatively large.

A fast convergent sum rule is the Gross–Llewellyn Smith (1969) sum rule

$$\begin{aligned} \int_0^1 [F_3^{\nu p}(x, Q^2) + F_3^{\bar{\nu}n}(x, Q^2)]dx &= 6 \left[ 1 - \frac{\alpha_s(Q^2)}{\pi} \right] \\ &= 5.4 \quad \text{at } Q^2 = 3 \text{ GeV}^2 \\ &= 5.00 \pm 0.16 \quad (\text{experiment}). \end{aligned} \quad (11.22)$$

The right-hand side includes first-order QCD corrections. Again the agreement is very good.

Finally, the integral  $\int_0^1 xq(x)dx$  gives the fraction of the proton's momentum carried by the  $q$  quark. Thus

$$\sum = \int_0^1 x[u(x) + d(x) + s(x) + \bar{u}(x) + \bar{d}(x) + \bar{s}(x)]dx = 0.54 \quad (11.23)$$

is the momentum carried by all the quarks inside the proton. This integral was determined by combining data from several processes. It is much less than unity, indicating that the quarks carry one half of the proton's momentum. The remaining half must be carried by other particles, which do not interact directly with the currents. They are the gluons of quantum chromodynamics.

## 11.2 Evolution of distribution functions

The algebraic relations discussed in this and the previous chapter assumed point-like constituents within the nucleon. We know from previous advances in physics that a particle that looks point-like on one resolution scale reveals substructure at a higher resolution. The scaling phenomenon and the numerous quantum-number relations revealed a point-like structure, but deviations from scaling indicate the existence of additional structure. In fact, it has been established that the variation of the structure functions with  $Q^2$  is due to the emission of vector particles: the gluons. As was mentioned earlier, they carry the other half of the momentum of the nucleons, that was missing in the momentum sum rule.

The additional structure is introduced by the theory of strong interactions known as quantum chromodynamics (QCD). There are many indications that each flavor of quarks comes in three colors: red, white, and blue. The names for the colors are arbitrary, but the fact that there are three is important. The quarks interact with each other by the exchange of vector bosons that change the color of the quarks.

The theory of the strong interaction – QCD – is a non-Abelian gauge theory based on the group  $SU(3)_c$ . Each quark species – up, down, strange, ... – forms a triplet in color space and has a coupling  $g_s$  to the eight gluons,  $G_\mu^\alpha$ , which belong to the adjoint representation of  $SU(3)$  color. We write the color triplet as

$$q(x) = \begin{pmatrix} q_r \\ q_w \\ q_b \end{pmatrix}$$

and the Lagrangian

$$\mathcal{L}_{\text{QCD}} = \bar{q}(x)i\gamma^\mu \left[ \partial_\mu + \frac{i}{2}g_s\lambda^\alpha G_\mu^\alpha(x) \right] q(x), \quad (11.24)$$

with  $\lambda^\alpha$  the Gell-Mann matrices of  $SU(3)_c$  and  $G_\mu^\alpha(x)$  with  $\alpha = 1, 2, \dots, 8$  the eight gluons. There is no mass term for the gluons that leaves the color symmetry exact. QCD makes dramatic predictions. The first one concerns the coupling constant.

In field theories coupling constants and other observables are modified by higher-order corrections that involve loops. Many loop diagrams are divergent, which demands special handling of them. When all the infinities from loop diagrams are absorbed into the definition of couplings, masses, and other parameters of the original Lagrangian, we say that the theory is renormalizable. In these theories we can calculate physical observables with high precision. QCD and the electroweak theory are renormalizable. It is beyond the scope of this book to describe or prove renormalization. Instead, we shall describe a few cases of higher-order corrections in order to demonstrate the methods entering these calculations. Furthermore, we describe some properties of field theories that have significant impact on properties of weak interactions.

One quantity modified by loop corrections is the strong coupling constant  $g_s$ . The infinities introduced by higher orders are absorbed into the redefinition of the coupling constant. Since the corrections involve the addition of infinite quantities, the numerical value of the coupling is unknown and must be determined experimentally. Thus  $\alpha_s$  is measured at a specific reference scale  $\mu_0$ , known as the renormalization point. In many cases the reference scale  $\mu$  is identified with the momentum flowing through the vertex. The arbitrariness of the reference point leads to a differential equation – the renormalization-group equation. To be specific, the change of  $\alpha(\mu) = g_s^2/(4\pi)$  with respect to the reference point  $\mu$  satisfies the equation

$$\mu \frac{d\alpha}{d\mu} = \beta(\alpha), \quad (11.25)$$

where  $\beta(\alpha)$  represents the sum of higher-order corrections and is of the form

$$\beta(\alpha) = \beta_0\alpha^3 + O(\alpha^5). \quad (11.26)$$

The constant  $\beta_0$  and higher terms are determined in perturbation theory. The solution is obtained as

$$\int_{\alpha(\mu_0)}^{\alpha(\mu)} \frac{d\alpha}{\beta(\alpha)} = \ln\left(\frac{\mu}{\mu_0}\right) \quad (11.27)$$

or, keeping the leading term on the right-hand side of Eq. (11.26), we obtain

$$\alpha(\mu) = \frac{\alpha(\mu_0)}{1 + \beta_0\alpha(\mu_0)\ln(\mu^2/\mu_0^2)}. \quad (11.28)$$

This states that, knowing the coupling constant at the reference scale  $\mu_0$ , we can predict its value at another scale  $\mu$ . The coupling constant is no longer a constant but runs with momentum; hence the name running coupling constant.

An important property of QCD is that the value of  $\beta_0 = 11 - \frac{2}{3}N_f$ , with  $N_f$  the number of generations, is positive. As the momentum increases, the coupling constant decreases and, at very high momentum,  $\alpha_s(p)$  is so small that perturbation theory is applicable. This provides a justification of scaling and of the parton model. It also goes beyond scaling, by predicting modifications introduced by the emission of gluons. The corrections are functions of  $Q^2$  producing predictable violations of scaling. The corrections have been studied extensively in perturbation theory and compared with many experimental results.

There is an extensive list of articles in which violations of scaling have been computed and are discussed in detail. Experimentally, the changes have been observed with the structure functions increasing for small  $x$  as functions of  $Q^2$  and decreasing for  $x > 0.4$ .

The second prediction concerns the production of gluons, which are emitted by the accelerating particles. The quarks produced materialize into hadrons and produce jets of particles. Similarly, the gluons also produce jets of hadrons. Consequently we expect some reactions to produce two jets (from  $q\bar{q}$  pairs) and others three jets (from  $q\bar{q}g$  production). Three-jet events have been observed in electron–positron-annihilation reactions. The production of gluons implies that they also exist within hadrons and are responsible for the missing momentum in the sum rule in Eq. (11.23). Consequently the experimental results have been analyzed with the inclusion of an additional distribution function for the gluons. A dramatic property of the gluon distribution function is its rapid increase at small  $x$ .

For small momenta the coupling constant grows and becomes very big, making a perturbative description impossible. It is customary to denote by  $\Lambda^2$  the scale of  $Q^2$  at which the denominator becomes zero. This happens at

$$\Lambda^2 = \mu_0^2 e^{-1/[\beta_0\alpha(\mu_0)]}. \quad (11.29)$$

It follows now that the coupling constant can be rewritten

$$\alpha(\mu) = \frac{1}{\beta_0 \ln(\mu^2/\Lambda^2)}. \quad (11.30)$$

We can think of  $\Lambda$  as the boundary between the region where quarks and gluons appear as quasi-free particles and the world of bound states like protons, pions, etc. At momenta smaller than  $\Lambda$ , the strong interaction becomes so strong that the quarks cannot come out as free particles, but remain confined within hadrons. This



property of confined quarks has not been proved yet, and thus it is difficult to judge which among several approaches may ultimately be the most productive.

It is evident that QCD and its consequences form an extensive and exciting topic, which is, however, beyond the scope of this book. We shall have occasion to return to QCD in Section 15.6, where we discuss the effective Hamiltonian for low-energy weak interactions. As a last topic concerning the charged-current interactions we discuss in the next section quasi-elastic scattering.

### 11.3 Quasi-elastic scattering

In contrast to deep inelastic scattering, quasi-elastic scattering gives information on the static properties of the proton and the neutron. In fact, the first experiments with neutrino beams measured the reactions shown in Fig. 11.2:

$$\nu(k) + n(p) \rightarrow \mu^-(k') + p(p'), \quad (11.31)$$

$$\bar{\nu}(k) + p(p) \rightarrow \mu^+(k') + n(p'), \quad (11.32)$$

which are still interesting on several accounts. For instance, we would like to determine their form factors accurately and check their relation to the electromagnetic form factors. Furthermore, the quasi-elastic cross sections reach constant values for neutrino energies greater than 2.0 GeV. This property has been used for measuring the flux of neutrino beams and is still useful. Low-energy neutrino interactions recently started being used efficiently for studying neutrino oscillations. For all these reasons we present in this chapter an explicit calculation.

For low energies relative to the mass of the W boson, interactions of neutrinos can be written as a leptonic current times a hadronic current:

$$\mathcal{M} = \frac{G}{\sqrt{2}} \bar{u}(k') \gamma_\mu (1 - \gamma_5) u(k) \langle p | J_\mu^+ | n \rangle.$$

The hadronic current has a complicated structure produced by the motion of the quarks within hadrons. We define the vector form factors of the charged current as

$$\langle p | V_\mu^+ | n \rangle = \bar{u}(p') \left( \gamma_\mu F_1^+ + i \frac{\sigma_{\mu\nu} q^\nu}{2M} F_2^+ + \frac{q_\mu}{M} F_3^+ \right) u(p). \quad (11.33)$$

Denoting, as before, the isovector form factor of the electromagnetic current by  $F_1^V$ , we obtain

$$F_1^+(q^2) = -2F_1^V(q^2). \quad (11.34)$$

The factor 2 comes from the normalization of  $V_\mu^+ = V_\mu^1 + iV_\mu^2$  and the Clebsch–Gordan coefficients, which are  $\sqrt{\frac{2}{3}}$  for the charged current and  $-\sqrt{\frac{1}{3}}$  for

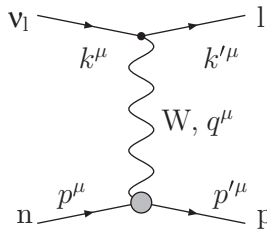


Figure 11.2. Quasi-elastic scattering.

the electromagnetic current. For the following calculation it is convenient to write the hadronic current in a modified form:

$$\langle p | J_\mu^+ | n \rangle = \bar{u}(p') \left[ g_V \gamma_\mu + f_V \frac{(p + p')_\mu}{2M} + h_V \frac{q_\mu}{2M} + g_A \gamma_\mu \gamma_5 + f_A i \sigma_{\mu\nu} \frac{q^\nu \gamma_5}{2M} + h_A \frac{q_\mu \gamma_5}{2M} \right] u(p), \quad (11.35)$$

where we left out the factor  $\cos \theta_c$  arising from the Cabibbo angle. In reducing (11.33) to (11.35) we used the Gordon decomposition formula, which gives the relations  $g_V = F_1^+ + F_2^+$ ,  $f_V = -F_2^+$ , and  $F_3^+$  vanishes as explained in Chapter 2. The term  $h_A q_\mu \gamma_5$  contributes to the cross section terms proportional to the lepton masses and will be omitted. In Chapters 1 and 2 we discussed the fact that charge conjugation and time-reversal together require  $h_V$  and  $f_A$  to vanish. On eliminating these three form factors, we obtain a simplified form for the matrix element which we shall use in this section:

$$\langle p | J_\mu^+ | n \rangle = \bar{u}(p') \left[ g_V \gamma_\mu + f_V \frac{(p + p')_\mu}{2M} + g_A \gamma_\mu \gamma_5 \right] u(p). \quad (11.36)$$

The electromagnetic form factors are known from electron-scattering experiments on protons and neutrons. Similar values of the axial form factor at low values of  $Q^2$  have been measured in  $\beta$ -decay. We shall use this information at the end of this section.

The calculation of the cross section is now straightforward but tedious. Since the calculation of quasi-elastic scattering is not easily available in books, I give a few intermediate steps. There is a second reason: the elastic scattering for neutral currents has a similar functional form that is obtained by replacing the form factors by those of neutral currents. Studies of quasi-elastic scattering frequently use a formula in terms of Mandelstam variables (Llewellyn Smith, 1974). We derive here two more formulas that are convenient for taking limits in specific kinematic regions.

The kinematics for the process are simplest in the laboratory frame where the nucleon is at rest:

$$\begin{aligned}
 p \cdot k &= p' \cdot k' = ME, \\
 p \cdot k' &= p' \cdot k = ME + \frac{q^2}{2}, \\
 k \cdot k' &= \frac{m_\mu^2}{2} - \frac{q^2}{2}, \\
 p \cdot p' &= \frac{M^2}{x} - \frac{q^2}{2}, \\
 Q^2 &= 2Mv = 4EE' \sin^2\left(\frac{\theta}{2}\right).
 \end{aligned}
 \tag{11.37}$$

The square of the hadronic tensor is obtained from (11.36)

$$\begin{aligned}
 H_{\mu\nu} &= (g_V^2 + g_A^2)(p_\mu p'_\nu + p_\nu p'_\mu - g_{\mu\nu} p \cdot p') - 2ig_V g_A \epsilon_{\mu\nu\gamma\delta} p^\gamma p'^\delta \\
 &+ M^2(g_V^2 - g_A^2)g_{\mu\nu} + \left(f_V^2 \frac{p \cdot p' + M^2}{4M^2} + f_V g_V\right)(p_\mu + p'_\mu)(p_\nu + p'_\nu).
 \end{aligned}
 \tag{11.38}$$

The first line of this equation follows from Eq. (8.37) and the remaining ones from a straightforward calculation. The similarities between Section 8.3 and the present one can be used for comparisons. For instance, the inner product of the leptonic tensor in Eq. (8.36) with  $H_{\mu\nu}$  leads to a matrix element that can be expressed in terms of the scattering angle. From the matrix element and the phase-space integral we arrive at the differential cross section

$$\begin{aligned}
 \frac{d\sigma}{dE'} &= \frac{G_F^2}{2\pi} M \frac{E'}{E} \left\{ (g_V^2 + g_A^2) \left[ 1 + \frac{Q^2}{2M^2} \sin^2\left(\frac{\theta}{2}\right) \right] + (g_A^2 - g_V^2) \sin^2\left(\frac{\theta}{2}\right) \right. \\
 &\left. - 2g_A g_V \left( \frac{E + E'}{M} \right) \sin^2\left(\frac{\theta}{2}\right) + \left[ f_V^2 \left( 1 + \frac{Q^2}{4M^2} \right) + 2f_V g_V \right] \cos^2\left(\frac{\theta}{2}\right) \right\}.
 \end{aligned}
 \tag{11.39}$$

Several limiting cases are now interesting. For  $g_A = 0$  the cross section depends only on the vector terms and the functional form agrees with the Rosenbluth formula. Differences between electroproduction and neutrino-induced formulas arise from the photon propagator and the coupling constants.

Alternatively, we may combine the  $g_V$  and  $g_A$  terms and obtain another expression for the cross section:

$$\frac{d\sigma}{dE'} = \frac{G_F^2 M}{4\pi} \left\{ (g_V - g_A)^2 + (g_V + g_A)^2 \left(\frac{E'}{E}\right)^2 + (g_A^2 - g_V^2) \frac{M\nu}{E^2} + \frac{1}{2} \left[ f_V^2 \left(1 + \frac{Q^2}{4M^2}\right) + 2f_V g_V \right] \left[ \left(1 + \frac{E'}{E}\right)^2 - \frac{Q^2}{E^2} \left(1 + \frac{Q^2}{4M^2}\right) \right] \right\}. \tag{11.40}$$

For  $f_V = 0$  the interaction of the neutrino has the same functional form as neutrino–electron scattering and the expression above agrees with Eq. (8.43).

The two equations for quasi-elastic scattering presented already are convenient for taking specific limits. It is customary, however, to use another formula, which expresses the differential cross section in terms of Mandelstam variables  $s$ ,  $u$ ,  $t = q^2$  (Llewellyn Smith 1974). Most recent analyses use it and have been able to account for the experimental data in terms of three form factors. The vector form factors are related to those measured in electromagnetic reactions. The axial form factor is parametrized

$$g_A(q^2) = \frac{g_A(0)}{(1 - q^2/M_A^2)^2}, \tag{11.41}$$

with  $g_A(0) = 1.26$  and  $M_A = 1.00 \pm 0.05 \text{ GeV}/c^2$  (its precise value is still being debated among the experts).

### References

Adler, S. L. (1965), *Phys. Rev.* **143**, 1144  
 Callan, C. G., and Gross, D. (1969), *Phys. Rev. Lett.* **22**, 156  
 Gross, D., and Llewellyn Smith, C. H. (1969), *Nucl. Phys.* **B14**, 337  
 Llewellyn Smith, C. H. (1974), *Phys. Rep.* **3C**, 264

### Select bibliography

Bjorken, J. D. and Paschos, E. A. (1970), *Phys. Rev.* **D1**, 3151  
 Feynman, R. P. (1972), *Photon–Hadron Interactions* (Reading, MA, W. A. Benjamin)